

Machine Learning the Cosmic Curvature in a Model-independent Way

Guo-Jian Wang,¹ Xiao-Jiao Ma,¹ and Jun-Qing Xia^{1*}

¹*Department of Astronomy, Beijing Normal University, Beijing 100875, China*

Accepted XXX. Received YYY; in original form ZZZ

ABSTRACT

In this work, we achieve the determination of the cosmic curvature Ω_K in a cosmological model-independent way, by using the Hubble parameter measurements $H(z)$ and type Ia supernovae (SNe Ia). In our analysis, two nonlinear interpolating tools are used to reconstruct the Hubble parameter, one is the Artificial Neural Network (ANN) method, and the other is the Gaussian process (GP) method. We find that Ω_K based on the GP method can be greatly influenced by the prior of H_0 , while the ANN method can overcome this. Therefore, the ANN method may have more advantages than GP in the measurement of the cosmic curvature. Based on the ANN method, we find a spatially open universe is preferred by the current $H(z)$ and SNe Ia data, and the difference between our result and the value inferred from Planck CMB is 1.6σ . In order to test the reliability of the ANN method, and the potentiality of the future gravitational waves (GW) standard sirens in the measurement of the cosmic curvature, we constrain Ω_K using the simulated Hubble parameter and GW standard sirens in a model-independent way. We find that the ANN method is reliable and unbiased, and the error of Ω_K is ~ 0.186 when 100 GW events with electromagnetic counterparts are detected, which is $\sim 56\%$ smaller than that constrained from the Pantheon SNe Ia. Therefore, the data-driven method based on ANN has potential in the measurement of the cosmic curvature.

Key words: cosmological parameters – cosmology: observations – methods: data analysis

1 INTRODUCTION

The cosmic curvature is a fundamental parameter in modern cosmology. Important problems, such as the evolution of the universe, the property of the dark energy, are closely related to the curvature of the universe. Theories of inflation predict that the radius of the curvature of the universe should be very large, which implies the cosmic curvature is very small. Therefore, the detection of a significant deviation from $\Omega_K = 0$ would have a profound impact on inflation models and fundamental physics. A lot of attention has been attracted to this issue (Eisenstein et al. 2005; Tegmark et al. 2006; Zhao et al. 2007; Wright 2007) and a flat universe is preferred by the latest Planck CMB experiment (Aghanim et al. 2018) with high precision: $\Omega_K = 0.0007 \pm 0.0019$ (68%, TT, TE, EE+lowE+lensing+BAO).

Although the cosmic curvature has been constrained with high precision, it should be stressed that almost all of these estimations assume some specific models of dark energy, such as the equation of state of $w(z)$. Thus, these

estimations are all model-dependent and indirect methods. It should be noted that there is degeneracy between the spatial curvature Ω_K and the equation of state parameter $w(z)$ of dark energy. This degeneracy makes it difficult to constrain these two parameters simultaneously, which hinder our understanding of the nature of dark energy. Therefore, cosmological model-independent estimations for the cosmic curvature will break the degeneracy and be helpful for studying the nature of dark energy.

Many works have been done to estimate cosmic curvature in a model-independent way. Bernstein (2006) proposed a model-independent method to constrain the cosmic curvature parameter Ω_K based on the sum rule of distances along null geodesics of the FLRW metric and it was put forward to test the validity of the FLRW metric (Räsänen et al. 2015). The Union2.1 SNe Ia (Suzuki et al. 2012) and strong gravitational lensing systems selected from the Sloan Lens ACS Survey (Bolton et al. 2008) were used in their analysis. However, the cosmic curvature was weakly constrained due to the large uncertainties of the gravitational lensing systems. Besides, the measurement of the cosmic curvature is not completely model-independent because the light curve

* E-mail: xiajq@bnu.edu.cn

fitting parameters of Union2.1 SNe Ia are determined by assuming the standard dark energy model with the equation of state being constant. Another model-independent method was proposed by Clarkson et al. (2007, 2008) to test the FLRW metric by combining the Hubble parameter measurements $H(z)$ and the transverse comoving distance $D_M(z)$. An important by-product of this method is that the cosmic curvature can be estimated if the FLRW metric is valid:

$$\Omega_k = \frac{[H(z)D'_M(z)]^2 - c^2}{[H_0 D_M(z)]^2}, \quad (1)$$

where H_0 is the Hubble constant, c is the speed of light, $D_M(z) = (1+z)D_A(z) = D_L(z)/(1+z)$ is the transverse comoving distance (Hogg 1999), and D'_M represents the derivative of D_M with respect to redshift z . This method has been widely used in the literature to test the FLRW metric or estimate the cosmic curvature (Shafieloo & Clarkson 2010; Mörtzell & Jönsson 2011; Li et al. 2014; Sapone et al. 2014; Yahya et al. 2014; Cai et al. 2016; Rana et al. 2016; Zheng et al. 2019; Li et al. 2019). However, the derivative of the transverse comoving distance to redshift, $D'_M(z)$, will introduce a large uncertainty.

Afterwards Yu & Wang (2016) proposed to estimate the cosmic curvature by combining the proper distance d_P and the transverse comoving distance D_M , which can avoid shortcomings of the methods mentioned above. The data used in their analysis is the Hubble parameter measurements $H(z)$ and the angular diameter distance d_A of baryon acoustic oscillation (BAO). However, their analysis is not completely model-independent because d_A and some of the $H(z)$ measurements are obtained from the BAO observations which are dependent on the assumed fiducial cosmological model. Furthermore, Li et al. (2016) and Wei & Wu (2017) proposed to constrain the cosmic curvature in a model-independent way by combining $H(z)$ and SNe Ia, and this method was applied to study the cosmic curvature and opacity (Wang et al. 2017). In addition, Wei (2018) proposed to test the cosmic curvature by using the Hubble parameter and future gravitational waves (GW), Liao (2019) proposed to constraint on the cosmic curvature with the lensing time delays and GW, Collett et al. (2019) proposed to constraint on the cosmic curvature with the lensing time delays and SNe Ia, and Wei & Melia (2019) proposed to constraint on the cosmic curvature using quasars and cosmic chronometers.

In most of these papers, the Gaussian process (GP) (Seikel et al. 2012a), a non-parametric smoothing method for reconstructing functions from data and is widely used in recent works (Bilicki & Seikel 2012; Seikel et al. 2012a,b; Shafieloo et al. 2012; Seikel & Clarkson 2013; Busti et al. 2014; Yahya et al. 2014; Yang et al. 2015; Cai et al. 2016; Wei & Wu 2017; Yu & Wang 2016; Zhang & Xia 2016; Wang et al. 2019), is used to construct a function of $H(z)$. However, Zhou & Li (2019) recently propose that the Gaussian process should be used with caution for $H(z)$ reconstruction. Moreover, Wei & Wu (2017) and Wang et al. (2017) also find that the Gaussian process is sensitive to the prior of the Hubble constant H_0 and the results are greatly influenced by H_0 . This may imply the unreliability of Gaussian process in the reconstruction of $H(z)$.

Recently, Wang et al. (2020) present a new non-parametric approach for reconstructing functions from data

using Artificial Neural Network (ANN) and a public code ReFANN¹ is developed. The ANN method has no assumption to the data and is a completely data-driven approach. In their analysis, the Hubble parameter can be reconstructed accurately without bias, and the function of $H(z)$ reconstructed by ANN can represent the actual distribution of the observational Hubble parameter and can be used for further estimations of cosmological parameters. More importantly, the reconstructed function of $H(z)$ is not sensitive to the Hubble constant. Thus, they proposed that the data-driven method based on ANN will be a very promising method in the reconstruction of functions from data.

In this work, we constraint on the cosmic curvature in a model-independent using the Hubble parameter measurements $H(z)$ and SNe Ia, without assuming any fiducial cosmology. In our analysis, two nonlinear interpolating tools, ANN and GP, are used to reconstruct the Hubble parameter. We test the performance of ANN and GP in the measurement of the cosmic curvature. In addition, we also test the capability of the future gravitational waves (GW) standard sirens in the measurement of the cosmic curvature.

This paper is organized as follows: In section 2, we reconstruct functions of the observational Hubble parameter using the ANN and GP methods. Section 3 present the application of the reconstructed function of $H(z)$ in the constraint on the cosmic curvature. In section 4, a discussion about the cosmic curvature is presented. Finally, a conclusion is shown in section 5.

2 RECONSTRUCTION OF $H(z)$

In this section, we reconstruct functions of Hubble parameter $H(z)$ using the ANN method and the GP method. We first introduce the Hubble parameter measurements and then achieve the reconstruction of $H(z)$.

2.1 Hubble parameter $H(z)$

The Hubble parameter measurements $H(z)$ that describe the expansion rate of the universe have been used for the exploration of the evolution of the universe and the nature of dark energy. $H(z)$ can be obtained in two ways. One method to obtain $H(z)$ is based on the detection of the radial BAO features (Gaztanaga et al. 2009; Blake et al. 2012; Samushia et al. 2013). However, the $H(z)$ data obtained using this method is based on an assumed fiducial cosmological model, which is not suitable for our model-independent analysis. Another method that obtains $H(z)$ is to calculate the differential ages of passively evolving galaxies at different redshifts, which provides the $H(z)$ measurements are cosmological model-independent (Jimenez & Loeb 2002) and can be used in our analysis. In this method, a change rate $\Delta z/\Delta t$ can be obtained, then the Hubble parameter $H(z)$ could be written as

$$H(z) \simeq -\frac{1}{1+z} \frac{\Delta z}{\Delta t}. \quad (2)$$

This method is usually called the cosmic chronometers, and the $H(z)$ data based on this method refers to as CC $H(z)$.

¹ <https://github.com/Guo-Jian-Wang/refann>

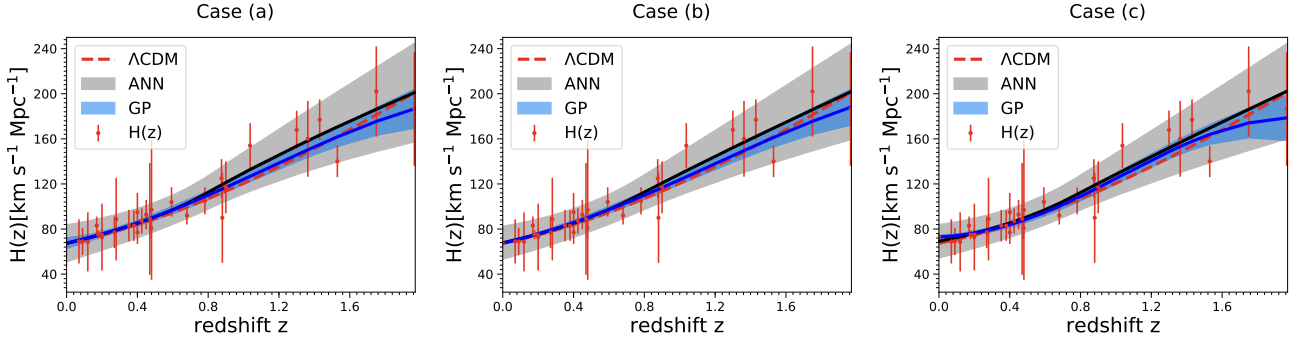


Figure 1. Reconstructed functions of $H(z)$ with ANN and GP. The red dots with error bars represent the $H(z)$ data, while the red dashed lines correspond to the flat Λ CDM models with $H_0 = 67.4 \text{ km s}^{-1} \text{ Mpc}^{-1}$ and $\Omega_m = 0.315$ (Planck2018 result).

The sample of CC $H(z)$ collected in Wang et al. (2020) is taken in our analysis, which has 31 data points totally in the redshift range of $[0.07, 1.965]$.

2.2 Function of CC $H(z)$

In our analysis, the cosmic curvature is constrained by comparing the distance modulus from $H(z)$ and that from SNe Ia. However, there is no corresponding $H(z)$ measurements on the redshift of each SNe Ia data point. One possible way is to reconstruct a function of $H(z)$ to ensure that there is a $H(z)$ measurement for each SNe Ia at the specific redshift. Therefore, we reconstruct a function of the CC $H(z)$ using ANN or GP to achieve the model-independent constraint on the cosmic curvature.

It should be noted that the minimum redshift of the CC $H(z)$ is 0.07, which is larger than most of the current SNe Ia data. Therefore, if we want to explore a lower redshift universe with the Hubble parameter, one possible way is to extend the reconstructed $H(z)$ function to a lower redshift. However, this extension is completely an approximation, which may introduce bias when having few $H(z)$ data in the vicinity of the redshift interval. Therefore, we consider a prior of the Hubble constant H_0 in the reconstruction of $H(z)$ to make the reconstructed function of $H(z)$ more reliable. Specifically, we adopt two recent measurements of H_0 in the reconstruction of $H(z)$: $H_0 = 67.4 \pm 0.5 \text{ km s}^{-1} \text{ Mpc}^{-1}$ with 0.7% uncertainty (Aghanim et al. 2018), and $H_0 = 73.24 \pm 1.74 \text{ km s}^{-1} \text{ Mpc}^{-1}$ with 2.4% uncertainty (Riess et al. 2016). Furthermore, for comparison, we also reconstruct $H(z)$ with no H_0 prior. Thus, there are 3 cases when reconstructing $H(z)$:

- (a) with no prior of H_0 ;
- (b) with a prior of $H_0 = 67.4 \pm 0.5 \text{ km s}^{-1} \text{ Mpc}^{-1}$; and
- (c) with a prior of $H_0 = 73.24 \pm 1.74 \text{ km s}^{-1} \text{ Mpc}^{-1}$.

For case (a), the sample has 31 observational Hubble parameters, and for cases (b) and (c), the sample contains an additional data point at the redshift $z = 0$, and thus has 32 data points for cases (b) and (c).

2.2.1 Reconstruction with ANN

When reconstructing a function from data with ReFANN, one should firstly tune hyperparameters of the neural net-

work to find an optimal ANN model (Wang et al. 2020). Here we adopt the optimal ANN model of reconstructing functions from Hubble parameter that is selected by Wang et al. (2020). The optimal model has one hidden layer with 4096 neurons in the hidden layer. Using this model, we reconstruct functions of $H(z)$ for these three $H(z)$ samples by training the ANN, and the results are shown in Figure 1 (the black solid lines with gray areas). The red dots with error bars represent the CC $H(z)$ and the red dashed line is the flat Λ CDM model with $H_0 = 67.4 \text{ km s}^{-1} \text{ Mpc}^{-1}$ and $\Omega_m = 0.315$ (Planck2018 result, Aghanim et al. (2018)).

We can see that the reconstructed functions of $H(z)$ are consistent with this flat Λ CDM model within a 1σ confidence level. Furthermore, the functions of $H(z)$ for these three cases are obviously consistent with each other within a 1σ confidence level. Specifically, for the best values of the reconstructed $H(z)$ (the black solid lines in Figure 1), the relative deviation of case (b) with respect to case (a) is $< 0.9\%$, and the relative deviation of case (c) with respect to case (a) is $< 2.0\%$. Therefore, this indicates that the function of $H(z)$ reconstructed by ANN is not sensitive to the prior of Hubble constant. Moreover, it should be noted that, for case (a), the reconstructed Hubble constant is

$$H_0 = 67.35 \pm 16.47 \text{ km s}^{-1} \text{ Mpc}^{-1}, \quad (3)$$

where the best-fit value is very similar to the latest Planck CMB result: $H_0 = 67.4 \pm 0.5 \text{ km s}^{-1} \text{ Mpc}^{-1}$, and is also consistent with that of Wang et al. (2020).

2.2.2 Reconstruction with GP

For comparison, we also reconstruct $H(z)$ with GP, and the python package GaPP (Seikel et al. 2012a) is used to execute the Gaussian process in our analysis. GaPP will reconstruct a function for the given data and return the mean and standard deviation of the reconstructed function at a specific redshift (Seikel et al. 2012a). In the Gaussian process, it is assumed to have correlation between the function value at x and the function value at some other point \tilde{x} , which is related by a covariance function. Therefore, when reconstructing functions with GP, it is necessary to select a specific covariance function. Here, we adopt the commonly used squared exponential covariance function:

$$k(x, \tilde{x}) = \sigma_f^2 \exp\left(-\frac{(x - \tilde{x})^2}{2\ell^2}\right), \quad (4)$$

where σ_f and ℓ are two hyperparameters that should be optimized. This function is infinitely differentiable and is the default setting of GaPP. We use the *dgp* function in GaPP to reconstruct functions from data. The two hyperparameters σ_f and ℓ are automatically optimized in this function.

The reconstructed functions of $H(z)$ are shown in Figure 1 with blue solid lines and areas. These $H(z)$ functions are consistent with the flat Λ CDM model (the red dashed lines) within a 1σ confidence level for cases (a) and (b), while a little deviation for case (c). This indicates that the prior of H_0 will greatly influence the reconstruction of $H(z)$ when using GP, which is slightly different from that of the ANN method. For the best values of the reconstructed $H(z)$ (the blue solid lines), the relative deviation of case (b) with respect to case (a) is $< 2.9\%$, and the relative deviation of case (c) with respect to case (a) is $< 15.3\%$ which is quite large. Moreover, for case (a), the reconstructed Hubble constant is

$$H_0 = 67.4 \pm 4.75 \text{ km s}^{-1} \text{ Mpc}^{-1}, \quad (5)$$

where the best-fit value is very similar to the latest *Planck* CMB result, and also similar to that of the ANN method (Equation 3).

3 COSMIC CURVATURE

In this section, we achieve the constraint on the cosmic curvature Ω_K by comparing the distance modulus of $H(z)$ and that obtained from the SNe Ia or GW. In section 3.1, we introduce the constraint on Ω_K using $H(z)$ and SNe Ia, and in section 3.2 we show the result constrained from $H(z)$ and GW.

3.1 Cosmic curvature from $H(z)$ & SNe Ia

3.1.1 SNe Ia data

The sample of SNe Ia used in our analysis is the latest Pantheon SNe Ia (Scolnic et al. 2018), which contains 1048 data points within the redshift range of $[0.01, 2.26]$. For these SNe Ia, two nuisance parameters, α and β , are recovered by using the BEAMS with Bias Corrections (BBC) method (Kessler & Scolnic 2017), and the corrected apparent magnitudes $m_{B,corr}^* = m_B^* + \alpha \times x_1 - \beta \times c + \Delta_B$ for all the SNe Ia are reported in (Scolnic et al. 2018), where Δ_B is a distance correction based on predicted biases from simulations. Therefore, the distance modulus of Pantheon SNe Ia can be rewritten as

$$\mu = m_{B,corr}^* - M_B, \quad (6)$$

where M_B represents the absolute magnitude of the B band that should be constrained simultaneously with the cosmological parameters. In the Pantheon sample, there is only one SNe (the SNe whose redshift is 2.26) exceeds the redshift range of the reconstructed function of $H(z)$. Thus, this SNe is not considered in our analysis, which means that there are only 1047 SNe Ia are taken in our analysis.

3.1.2 Method

In section 2.2, we reconstruct functions of CC $H(z)$ using the ANN and GP methods. Then, the total line-of-sight comov-

Table 1. 1σ Constraints on Ω_K constrained from $H(z)$ and Pantheon SNe Ia. The $H(z)$ is reconstructed by using the ANN method. Case (a), (b) and (c) represent no prior of H_0 , $H_0 = 67.74 \pm 0.46 \text{ km s}^{-1} \text{ Mpc}^{-1}$, and $H_0 = 73.24 \pm 1.74 \text{ km s}^{-1} \text{ Mpc}^{-1}$ when reconstructing the function of $H(z)$, respectively. See the text for details.

Cases	(a)	(b)	(c)
Ω_K	0.665 ± 0.419	0.626 ± 0.340	0.461 ± 0.349

ing distance D_C (Hogg 1999) can be further derived from the reconstructed functions of $H(z)$ by using

$$D_C = c \int_0^z \frac{dz'}{H(z')}, \quad (7)$$

where the error of D_C is obtained by integrating the error of the function of $H(z)$. Furthermore, the luminosity distance D_L can be obtained from D_C via

$$\frac{D_L}{(1+z)} = \begin{cases} \frac{D_H}{\sqrt{\Omega_K}} \sinh[\sqrt{\Omega_K} D_C/D_H] & \Omega_K > 0 \\ D_C & \Omega_K = 0 \\ \frac{D_H}{\sqrt{|\Omega_K|}} \sin[\sqrt{|\Omega_K|} D_C/D_H] & \Omega_K < 0, \end{cases} \quad (8)$$

where $D_H = cH_0^{-1}$. The reconstructed distance modulus μ_H can be further obtained by using

$$\mu_H = 5 \log \frac{D_L}{\text{Mpc}} + 25, \quad D_L = (1+z)D_C, \quad (9)$$

and the corresponding errors can be propagated by using

$$\sigma_{\mu_H} = \frac{5}{\ln 10} \frac{\sigma_{D_L}}{D_L}, \quad \sigma_{D_L} = (1+z)\sigma_{D_C}. \quad (10)$$

Finally, the cosmic curvature Ω_K can be constrained by minimizing the χ^2 statistic,

$$\chi^2 = \Delta\hat{\mu}^T \cdot \mathbf{Cov}^{-1} \cdot \Delta\hat{\mu}, \quad (11)$$

where $\Delta\hat{\mu} = \hat{\mu}_{\text{SNe}} - \hat{\mu}_H$ is the difference between the distance modulus of SNe Ia and that of the $H(z)$ data, and \mathbf{Cov} is the full covariance matrix. For the Pantheon SNe Ia, the BBC method produces distances from the fit parameters directly, thus, there is only a single systematic covariance matrix \mathbf{C}_{sys} .

3.1.3 Ω_K from ANN

Using the Markov chain Monte Carlo (MCMC) method, the best-fit value and uncertainty of the cosmic curvature can be obtained by generating sample points of the probability distribution to Ω_K and other nuisance parameters simultaneously. One-dimensional distribution of Ω_K constrained from $H(z)$ +Pantheon is shown in the left panel of Figure 2, and the corresponding best-fit value with 1σ errors are listed in Table 1. The black solid, dashed and dotted lines referring to the result of case (a), (b) and (c), respectively. We can see that the results of cases (b) and (c) are a little different from that of the case (a), which should be caused by the prior of H_0 in the reconstruction of $H(z)$. However, the results of these three cases are consistent with each other within a 1σ confidence level, and all of them favor a positive value of Ω_K , and the differences between these three results and the value inferred from Planck CMB are 1.6σ , 1.8σ , and

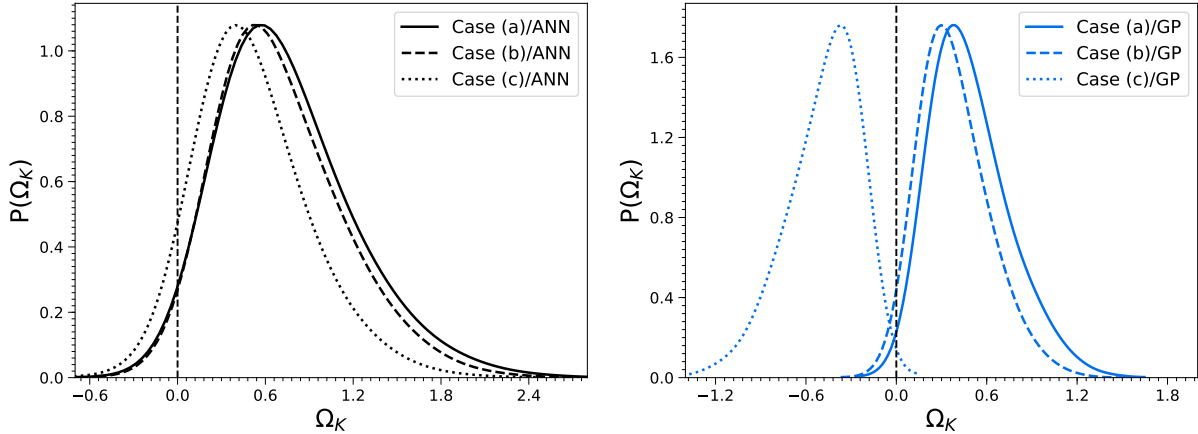


Figure 2. One-dimensional marginalized distribution of Ω_K constrained from $H(z)$ and Pantheon SNe Ia. *Left:* the $H(z)$ is reconstructed by using the ANN method. *Right:* the $H(z)$ is reconstructed by using the GP method.

Table 2. The same as Table 1, but now the $H(z)$ is reconstructed by using the GP method.

Cases	(a)	(b)	(c)
Ω_K	0.447 ± 0.248	0.348 ± 0.217	-0.440 ± 0.234

1.3 σ , respectively. Therefore, a spatially open universe may be preferred by $H(z)$ and Pantheon SNe Ia.

In addition, we can see that the best-fit value of case (a) is similar to that of case (b), while for case (c), the best-fit value is a little smaller than that of cases (a) and (b). This is not difficult to understand, because the reconstructed Hubble constant (Equation 3) of the case (a) is similar to the prior of H_0 in case (b). Furthermore, the consistency of the results of these three cases within a 1 σ confidence level may indicate that the ANN method is capable to extend the reconstructed $H(z)$ function to a lower redshift to enable explore a lower redshift universe with the Hubble parameter. Thus, the prior of the Hubble constant does not have a significant effect on the estimation of the cosmic curvature.

3.1.4 Ω_K from GP

Following the same procedure of section 3.1.2, the total line-of-sight comoving distance D_C can be derived from the functions of $H(z)$ reconstructed by GP, then the the luminosity distance D_L can be further obtained from D_C , and finally the distance modulus can be calculated by using D_L . Then, the cosmic curvature Ω_K can be constrained by minimizing the χ^2 statistic of Equation 11.

The cosmic curvature constrained from $H(z)$ +Pantheon are listed in Table 2 and the one-dimensional marginalized distribution of Ω_K is shown in the right panel of Figure 2. We can see the result of the case (a) is similar to that of the case (b), and both them favor a positive value of Ω_K , and the differences of the results and that inferred from the Planck CMB are 1.8 σ and 1.6 σ . However, the result of the case (c) favors a negative value of Ω_K and the difference of the result and that of Planck CMB is 1.9 σ , which is statistically quite different from that

of cases (a) and (b). These results indicate that the prior of H_0 will greatly influence the measurement of the cosmic curvature when using GP.

Moreover, we can see that the results of cases (a) and (b) are consistent with that obtained using the ANN method within a 1 σ confidence level. However, it is quite different for case (c), and the difference between the result and that based on the ANN method is 2.1 σ . Therefore, comparing the results of sections 3.1.3, we can see that the cosmic curvature based on the ANN method is more stable than that based on the GP method, which may indicate that the ANN method will surpass the GP method in the measurement of the cosmic curvature.

3.2 Cosmic curvature from $H(z)$ & GW

The positive value of Ω_K preferred by the current CC $H(z)$ and SNe Ia data is contrary to the flat universe supported by CMB experiments in Λ CDM model. Any deviation from $\Omega_K = 0$ would have a profound impact on inflation models and fundamental physics. Thus, this result should be taken seriously and tested strictly. Therefore, in order to further test the reliability of the ANN method, and the potentiality of GW in the estimation of the cosmic curvature, we constrain Ω_K using the simulated Hubble parameter and GW standard sirens in a model-independent way. We first introduce the simulation of GW standard sirens and then achieve the estimation of the cosmic curvature.

3.2.1 GW standard sirens

The chirping GW signals from inspiralling compact binaries can provide an absolute measure of the luminosity distance because the amplitude of GW depends on the so-called chirp mass and the luminosity distance. The chirp mass is measured from the phasing of GW, thus, the luminosity distance D_L can be extracted from the amplitude, which makes GW known as standard siren (Schutz 1986; Abbott et al. 2017). Besides, if the compact binaries are black hole-neutron star (BH-NS) or binary neutron stars (NS-NS), the redshift of GW sources can be obtained from its electromagnetic coun-

terpart (EM). Therefore, this offers a model-independent way to establish the $D_L - z$ relation over a wide range of redshift and thus can be used in our model-independent estimation of the cosmic curvature.

The GW events used here is simulated from the Einstein Telescope (ET), a third generation gravitational wave detector that is designed with high-sensitivity and wide frequency range ($1 - 10^4$ Hz), and would be able to detect the NS-NS mergers up to the redshift of $z \sim 2$ and BH-NS mergers up to $z > 2$ (Punturo et al. 2010). We firstly generate the redshift of the GW events. The redshift distribution of GW events is taken to has the form of (Zhao et al. 2011)

$$P(z) \propto \frac{4\pi D_C^2(z)R(z)}{H(z)(1+z)}, \quad (12)$$

where D_C is the total line-of-sight comoving distance and $R(z)$ describes the time evolution of the burst rate with the form (Schneider et al. 2001; Cutler & Holz 2009)

$$R(z) = \begin{cases} 1 + 2z, & z \leq 1 \\ \frac{3}{4}(5 - z), & 1 < z < 5 \\ 0, & z \geq 5. \end{cases} \quad (13)$$

The redshift of GW events is simulated according to this distribution. Then we calculate the luminosity distance in a flat Λ CDM model using

$$D_L(z) = \frac{c(1+z)}{H_0} \int_0^z \frac{dz}{\sqrt{\Omega_m(1+z)^3 + \Omega_K(1+z)^2 + \Omega_\Lambda}}, \quad (14)$$

where $\Omega_\Lambda = 1 - \Omega_m - \Omega_K$ and the fiducial $H_0 = 70 \text{ km s}^{-1} \text{ Mpc}^{-1}$, $\Omega_m = 0.3$ and $\Omega_K = 0$.

Then the uncertainty of the luminosity distance σ_{D_L} of GW events is simulated by following the simulation process of Cai & Yang (2017). The total uncertainty of luminosity is

$$\sigma_{D_L} = \sqrt{(\sigma_{D_L}^{\text{inst}})^2 + (\sigma_{D_L}^{\text{lens}})^2} \quad (15)$$

where $\sigma_{D_L}^{\text{inst}}$ is the instrumental error of the luminosity distance, and $\sigma_{D_L}^{\text{lens}}$ is the additional error due to the weak lensing which is assumed to be $\sigma_{D_L}^{\text{lens}}/D_L = 0.05z$. For the simulation of $\sigma_{D_L}^{\text{inst}}$, we refer the reader to Cai & Yang (2017) for the detailed process (see also Zhao et al. (2011); Wei (2018); Qi et al. (2019)). The mass distribution is chosen uniformly in the interval $[1, 2]M_\odot$ for neutron stars and $[3, 10]M_\odot$ for black holes. As the argument in (Cai & Yang 2017), the ET is expected to detect $\mathcal{O}(10^2)$ GW events with EM counterparts per year, and the ratio of possibly detecting BH-NS and NS-NS events is assumed to be 0.03. Thus we firstly simulate 100 GW events, shown in Figure 3. Note that the maximum redshift of the observational $H(z)$ is ~ 2 , therefore, we only simulate the GW events in $0 < z < 2$.

3.2.2 Constraint on Ω_K

In our analysis, 100 $H(z)$ is simulated with the same fiducial model (Equation 14) by using the method illustrated in Wang et al. (2020). Using the mock data of $H(z)$ and GW events, we can test the capability of GW to the constraint on the cosmic curvature, as well as the reliability of the ANN method. With the simulated luminosity distance

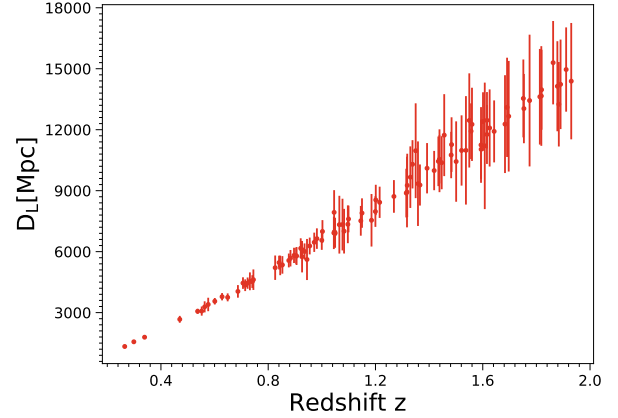


Figure 3. The simulated luminosity distances of 100 GW events observed by ET.

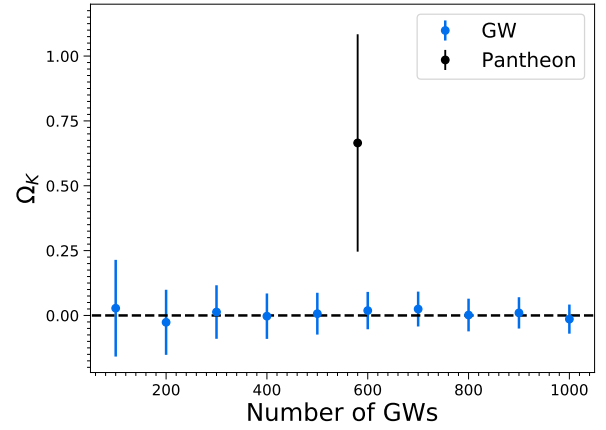


Figure 4. Best-fit cosmic curvature Ω_K and 1σ confidence level as a function of the number of GW events. The black dashed line represents the fiducial flat universe.

of GW events, we can further obtain the distance modulus μ_{GW} using Equation 9 and the corresponding errors can be propagated from that of D_L by using

$$\sigma_{\mu_{GW}} = \frac{5}{\ln 10} \frac{\sigma_{D_L}}{D_L}. \quad (16)$$

Then we can constrain the cosmic curvature Ω_K by minimize the χ^2

$$\chi^2(\Omega_K) = \sum_i \frac{[\mu_H(z_i; \Omega_K) - \mu_{GW}(z_i)]^2}{\sigma_{\mu_H, i}^2 + \sigma_{\mu_{GW}, i}^2}. \quad (17)$$

Specifically, we firstly reconstruct a function of $H(z)$ using the ANN method, then integrate it to obtain the modulus distance μ_H , and finally achieve the estimation of the cosmic curvature using Equation 17. The cosmic curvature constrained from the simulated $H(z)$ and 100 GW events is

$$\Omega_K = 0.028 \pm 0.186. \quad (18)$$

This result is consistent with the fiducial value of $\Omega_K = 0$ within a 1σ confidence level, which implies the reliability of the ANN method. Moreover, we note that the error of this result is about 56% smaller than that constrained using Pantheon SNe Ia (case (a) in Table 1). Therefore, the GW

standard siren will be a powerful tool in the constraint on the cosmic curvature.

In order to show how effective of the GW standard siren in the constraint on Ω_K , we further simulate several catalogs of GW events with the number varies from 200 to 1000 and use them to constrain the cosmic curvature. The best-fit values of Ω_K and the corresponding errors as a function of the number of GW events are shown in Figure 4. We can see that the error of Ω_K decrease with the increase in the number of GW events and all these results are consistent with the fiducial flat universe within a 1σ confidence level. In addition, the error of Ω_K will be 0.056 when 1000 GW events are detected, which is much smaller than that obtained from SNe Ia. Therefore, the Hubble parameter and future gravitational wave standard siren will constrain the cosmic curvature Ω_K in a model-independent way with high precision.

For the ten sets of constraint on Ω_K , the average relative deviation from the fiducial flat universe is 0.07σ , which is quite small. For comparison, we also reconstruct the Hubble parameter with the GP method, and obtain another ten sets of constraint on Ω_K . The corresponding average relative deviation from the fiducial flat universe is 0.52σ . This deviation is much larger than that based on ANN. Therefore, this indicates that the ANN method will surpass the GP method in the measurement of the cosmic curvature.

4 DISCUSSIONS

In section 3.1.3, with the function of $H(z)$ reconstructed with the ANN method, we show that a positive value of Ω_K is favored by the current CC $H(z)$ and Pantheon SNe Ia. The analysis of Wang et al. (2020) and section 3.2.2 show that the ANN method is reliable and unbiased for both the best-fit values and errors of the reconstructed functions of $H(z)$, thus, the constraint on the cosmic curvature should be reliable. However, it should be noted that the cosmic curvature Ω_K is strongly degenerate with the absolute magnitude M_B of SNe Ia (see Figure 5), which means that a small deviation of the absolute magnitude will lead to a great change in the cosmic curvature. Thus, this degeneracy may makes it difficult to constrain the cosmic curvature and the nuisance parameters of SNe Ia simultaneously and prevents us from understanding the nature of the cosmic curvature. Moreover, the Hubble parameters used in this work have only 31 observations, which is much smaller than that of SNe Ia. Thus, the number of the current CC $H(z)$ may not be sufficient to represent the actual situation of the Hubble parameters. Therefore, further analysis is needed with more Hubble parameter observations.

5 CONCLUSIONS

In this work, we reconstruct functions of CC $H(z)$ with the ANN and GP methods and integrate them to obtain the distance modulus μ_H . Then we constrain the cosmic curvature Ω_K by comparing μ_H and the distance modulus obtained from Pantheon SNe Ia. We find that the function of $H(z)$ reconstructed by GP can be greatly influenced by the prior of the Hubble constant. However, the ANN method

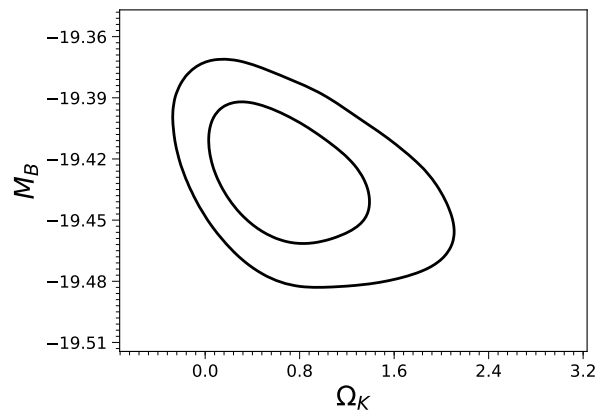


Figure 5. Two-dimensional marginalized distribution for Ω_K and M_B .

can overcome this to reduce the influence of the prior of the Hubble constant on the function of $H(z)$, and further reduce the influence on the measurement of the cosmic curvature. Therefore, the ANN method may surpass the GP method in the measurement of the cosmic curvature.

Based on the ANN method, we find a positive value of Ω_K is favored by the current CC $H(z)$ and Pantheon SNe Ia data, and the difference between this result and that obtained using Planck CMB is 1.6σ . In order to test the reliability of the ANN method in the measurement of the cosmic curvature, we further constrain the cosmic curvature in a model-independent way, by using the simulated Hubble parameter and the GW standard sirens that from the Einstein Telescope. We find the ANN method is reliable and unbiased, and thus the deviation of the cosmic curvature from the flat universe is no caused by the ANN method.

Moreover, the results show that the error of Ω_K is ~ 0.186 when 100 GW events with electromagnetic counterparts are detected, which is $\sim 56\%$ smaller than that constrained from the $H(z)$ and Pantheon SNe Ia, and ~ 0.056 when having 1000 GW events with electromagnetic counterparts. Therefore, the data-driven method based on ANN has potential in the measurement of the cosmic curvature when using the future Hubble parameter and GW standard siren.

6 ACKNOWLEDGEMENT

We thank Zhengxiang Li and Jingzhao Qi for helpful discussions. J.-Q. Xia is supported by the National Science Foundation of China under grants No. U1931202, 11633001, and 11690023; the National Key R&D Program of China No. 2017YFA0402600.

REFERENCES

- Abbott, B. P., Abbott, R., Adhikari, R. X., et al. 2017, *Nature*, **551**, 85
- Aghanim, N. et al. [Planck Collaboration], 2018, *arXiv:1807.06209*
- Bernstein, G. 2006, *ApJ*, **637**, 598
- Bilicki, M., & Seikel, M. 2012, *MNRAS*, **425**, 1664

Blake, C., Brough, S., Colless, M., et al. 2012, *MNRAS*, **425**, 405

Bolton, A. S., Burles, S., Koopmans, L. V. E., et al. 2008, *ApJ*, **682**, 964

Busti, V. C., Clarkson, C., & Seikel, M. 2014, *MNRAS*, **441**, L11

Cai, R.-G., Guo, Z.-K., & Yang, T., 2016, *PRD*, **93**, 043517

Cai, R.-G. and Yang, T., 2017, *Physical Review D* **95**, 044024

Clarkson, C., Cortes, M., & Bassett, B., *JCAP*, **2007**, **08**, 011

Clarkson, C., Bassett, B. A., & Hui-Ching Lu, T., 2008, *PRL*, **101**, 011301

Collett, T., Montanari, F., Rasanen, S., 2019, *Phys. Rev. Lett.* **123**, 231101

Cutler, C. and Holz, D. E., 2009, *Phys. Rev. D* **80**, 104009

Eisenstein, D. *et al.* (SDSS Collaboration), 2005, *Astrophys. J.* **633**, 560

Gaztañaga, E., Cabré, A., & Hui, L. 2009, *MNRAS*, **399**, 1663

Hogg, D. W., 1999, *arXiv:astro-ph/9905116*

Jimenez, R., & Loeb, A. 2002, *ApJ*, **573**, 37

Kessler, R., & Scolnic, D. 2017, *ApJ*, **836**, 56

Li, S.-Y., Li, Y.-L., Zhang, T.-J., Zhang, T., 2019, *arXiv:1910.09794*

Li, Y.-L., Li, S.-Y., Zhang, T.-J., & Li, T.-P. 2014, *ApJL*, **789**, L15

Li, Z., Wang, G.-J., Liao, K., & Zhu, Z.-H. 2016, *ApJ*, **833**, 240

Liao, K., 2019, *Phys. Rev. D* **99**, 083514

Mörtsell, E., & Jönsson, J., 2011, *arXiv:1102.4485*

Punturo, M., Abernathy, M., Acernese, F., & et al. 2010, *Classical and Quantum Gravity*, **27**, 194002

Qi, Jing-Zhao, Cao, Shuo, Pan, Yu, and Li, Jin, 2019, *arXiv:1902.01702*

Rana, A., Jain, D., Mahajan, S., Mukherjee, A., 2016, *JCAP*, **07**, 026

Räsänen, S., Bolejko, K., & Finoguenov, A., 2015, *PRL*, **115**, 101301

Riess, A. G., Macri, L. M., Hoffmann, S. L., et al. 2016, *ApJ*, **826**, 56

Samushia, L., Reid, B. A., White, M., et al. 2013, *MNRAS*, **429**, 1514

Sapone, D., Majerotto, E., & Nesseris, S., 2014, *PRD*, **90**, 023012

Schneider, R., Ferrari, V., Matarrese, S., and Portegies Zwart, S. F., 2001, *MNRAS*, **324**, 797

Schutz, B. F. 1986, *Nature*, **323**, 310

Scolnic, D. M., Jones, D. O., Rest, A., et al. 2018, *ApJ*, **859**, 101

Seikel M., Clarkson C. and Smith M., 2012a, *JCAP*, **06**, 036

Seikel, M., Yahya, S., Maartens, R., & Clarkson, C. 2012b, *Phys. Rev. D*, **86**, 083001

Seikel, M., & Clarkson, C., 2013, *arXiv:1311.6678*

Shafieloo, A. & Clarkson, C., 2010, *PRD*, **81**, 083537

Shafieloo, A., Kim, A. G., & Linder, E. V. 2012, *Phys. Rev. D*, **85**, 123530

Suzuki, N., Rubin, D., Lidman, C., et al. 2012, *ApJ*, **746**, 85

The Einstein Telescope Project, <https://www.etgw.eu/et/>

Tegmark, M. *et al.* (SDSS Collaboration), 2006, *Phys. Rev. D* **74**, 123507

Wang, D, Zhang, W, Meng, X-H, 2019, *Eur.Phys.J. C* **79** (2019) no.3, 211

Wang, G.-J., Wei, J.-J., Li, Z.-X., et al. 2017, *ApJ*, **847**, 45

Wang, G.-J., Ma, X.-J., Li, S.-Y., Xia, J.-Q. 2020, *ApJS*, **246**, 13

Wei, J.-J. & Wu, X.-F., 2017, *ApJ*, **838**, 160w

Wei, J.-J. 2018, *ApJ*, **868**, 29

Wei, J.-J., Melia, F., 2019, *arXiv:1912.00668*

Wright, E. L., 2007, *Astrophys. J.* **664**, 633

Yahya, S., Seikel, M., Clarkson, C., Maartens, R., & Smith, M. 2014, *PhRvD*, **89**, 023503

Yang, T, Guo, Z-K, Cai, R-G, 2015, *PRD*, **91**, 123533

Yu, H., & Wang, F. Y. 2016, *ApJ*, **828**, 85

Zhang, M.-J., & Xia, J.-Q., 2016, *JCAP*, **12**, 005Z

Zhao, G. B., Xia, J. Q., Li, H., Tao, C., Virey, J. M. , Zhu, Z. H. , and X. Zhang, 2007, *Phys. Lett. B* **648**, 8

Zhao, W., Van Den Broeck, C., Baskaran, D. and Li, T. G. F., 2011, *Physical Review D* **83**, 023005

Zheng, J., Melia, F., Zhang, T.-J., 2019, *arXiv:1901.05705*

Zhou, H., & Li, Z., 2019, *Chinese Physics C.*, **43**, 035103

This paper has been typeset from a \LaTeX file prepared by the author.